Deformation band clusters on Mars and implications for subsurface fluid flow

Chris H. Okubo[†]
Lunar and Planetary Laboratory, The University of Arizona, 1541 East University Boulevard, Tucson, Arizona 85721, USA

Richard A. Schultz
Geomechanics–Rock Fracture Group, Department of Geological Sciences/172, Mackay School of Earth Sciences and Engineering, University of Nevada, Reno, Nevada 89557, USA

Marjorie A. Chan
Department of Geology & Geophysics, University of Utah, 135 S. 1460 E, Salt Lake City, Utah 84112, USA

Goro Komatsu
International Research School of Planetary Sciences, Università d'Annunzio, Viale Pindaro 42, 65127 Pescara, Italy

High-Resolution Imaging Science Experiment (HiRISE) Team
Lunar and Planetary Laboratory, The University of Arizona, 1541 East University Boulevard, Tucson, Arizona 85721, USA

ABSTRACT

High-resolution imagery reveals unprecedented lines of evidence for the presence of deformation band clusters in layered sedimentary deposits in the equatorial region of Mars. Deformation bands are a class of geologic structural discontinuity that is a precursor to faults in clastic rocks and soils. Clusters of deformation bands, consisting of many hundreds of individual subparallel bands, can act as important structural controls on subsurface fluid flow in terrestrial reservoirs, and evidence of diagenetic processes is often preserved along them. Deformation band clusters are identified on Mars based on characteristic meter-scale architectures and geologic context as observed in data from the High-Resolution Imaging Science Experiment (HiRISE) camera. The identification of deformation band clusters on Mars is a key to investigating the migration of fluids between surface and subsurface reservoirs in the planet's vast sedimentary deposits. Similar to terrestrial examples, evidence of diagenesis in the form of light- and dark-toned discoloration and wall-rock induration is recorded along many of the deformation band clusters on Mars. Therefore, these structures are important sites for future exploration and investigations into the geologic history of water and water-related processes on Mars.

Keywords: deformation band, fault, fluid flow, diagenesis, Mars.

INTRODUCTION

Faults and other structural discontinuities can act as important controls on fluid flow in terrestrial reservoirs. The mechanics of deformation band formation have been discussed at length in many previous works (e.g., Wong et al., 1997; Schultz and Siddharthan, 2005; Aydin et al., 2006; Fossen et al., 2007), and thus only a brief overview is provided here. Deformation bands are tabular structural discontinuities (Aydin et al., 2006; Schultz and Fossen, 2008) that form through localized inelastic strain in porous and granular materials. The process of deformation band formation is commonly quantified in terms of the mean and differential driving stresses using a capped strength envelope (e.g., Schultz and Siddharthan, 2005; Aydin et al., 2006).

Deformation bands form through inelastic shear and involve varying amounts of either dilation or compaction of the host rock, depending on the magnitudes of the causative driving stresses. Localized inelastic dilation occurs under mean driving stresses that are either tensile or slightly compressive. Larger magnitudes of mean stress lead to inelastic compaction. Strain along deformation bands is accommodated through localized changes in porosity, grain rolling, and grain crushing within the tabular thickness of the band (Aydin, 1978; Wong et al., 1997; Schultz and Siddharthan, 2005; Aydin et al., 2006). Deformation bands do not form through frictional slip but instead create the necessary discontinuities along which frictional slip can occur (Aydin and Johnson, 1978; Schultz and Balasko, 2003; Schultz and Siddharthan, 2005; Aydin et al., 2006).

Individual deformation bands typically have widths on the order of one to several millimeters and have meter-scale lengths (Fig. 1A; Aydin, 1978; Eichhubl et al., 2004; Fossen et al., 2007). Deformation bands often occur in clusters consisting of many hundreds of individual subparallel bands, and these clusters can attain widths on the order of several meters and lengths of several hundred meters to kilometers (Figs. 1B and 1C; Aydin and Johnson, 1978; Antonellini and Aydin 1995; Fossen et al., 2005; Shipton et al., 2005; Okubo and Schultz, 2005).

Deformation bands are commonly classified according to the sense of volumetric strain (dilation or compaction) that is accommodated within the tabular thickness of the band. The relative magnitude of shear strain along the band can be used as an additional classification metric (Fossen et al., 2007). For the purposes of this paper, simple kinematic classifications based on the sense of volumetric strain alone, e.g., "dilational shear band" and "compactional shear band," are sufficient.

[†]E-mail: cokubo@usgs.gov. Present address: U.S. Geological Survey, 2255 N. Gemini Drive, Flagstaff, Arizona 86001, USA.

GSA Bulletin; March/April 2009; v. 121; no. 3/4; p. 474–482; doi: 10.1130/B26421.1; 8 figures; Data Repository item 2008191.

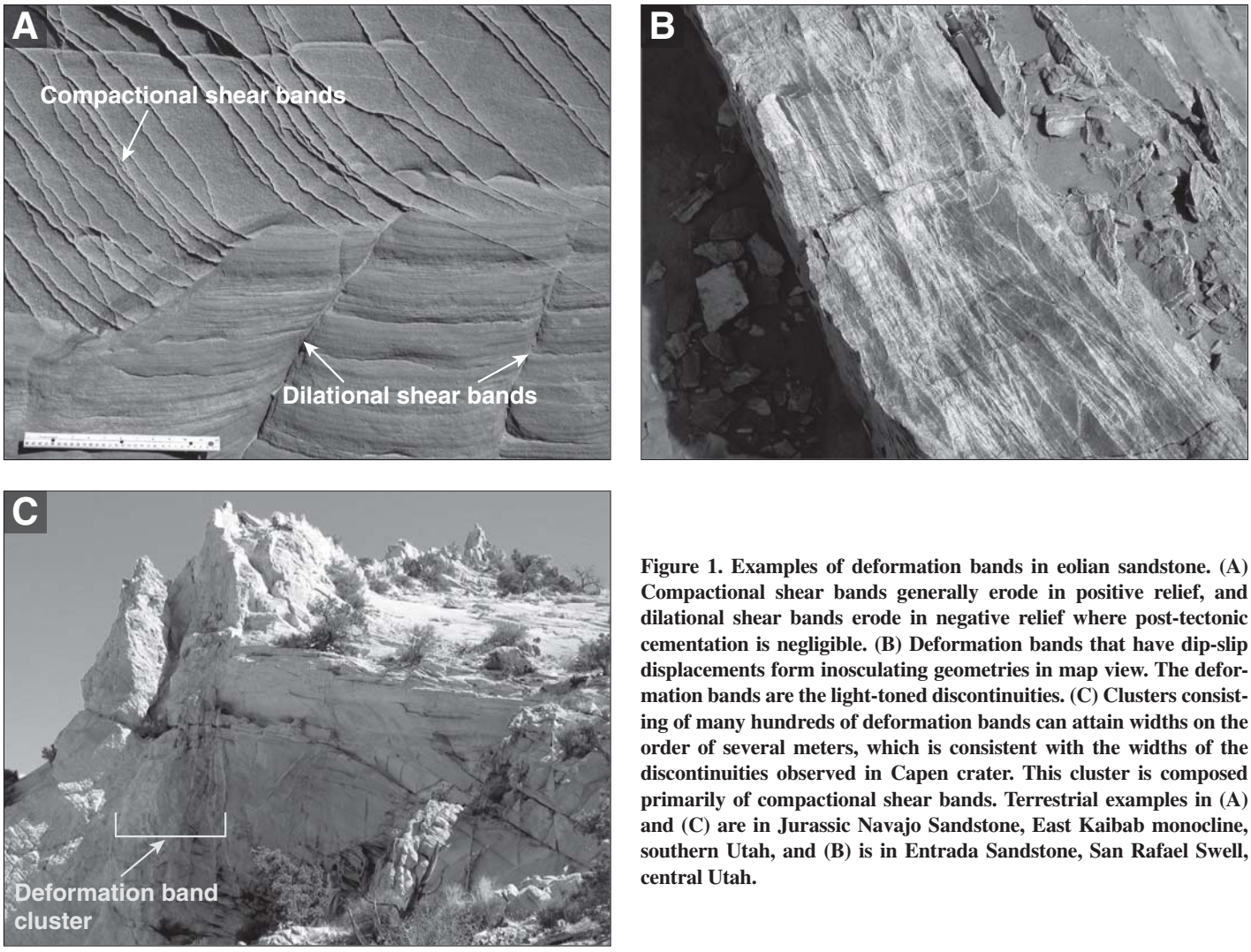

Figure 1. Examples of deformation bands in eolian sandstone. (A) Compactional shear bands generally erode in positive relief, and dilational shear bands erode in negative relief where post-tectonic cementation is negligible. (B) Deformation bands that have dip-slip displacements form inosculating geometries in map view. The deformation bands are the light-toned discontinuities. (C) Clusters consisting of many hundreds of deformation bands can attain widths on the order of several meters, which is consistent with the widths of the discontinuities observed in Capen crater. This cluster is composed primarily of compactional shear bands. Terrestrial examples in (A) and (C) are in Jurassic Navajo Sandstone, East Kaibab monocline, southern Utah, and (B) is in Entrada Sandstone, San Rafael Swell, central Utah.

Clusters of deformation bands can act as either conduits or baffles to fluid flow depending on the sense of strain accommodated along the bands and permeability contrast with the host rock (e.g., Antonellini and Aydin 1994, 1995; Taylor and Pollard, 2000; Ogilvie and Glover, 2001; Shipton et al., 2005; Fossen et al., 2007), although not all deformation bands show a strong control on fluid flow (e.g., Fossen and Bale, 2007). The permeability of individual compactional shear bands can be one to three orders of magnitude less than the nondeformed host rock, while dense clusters of these bands can exhibit up to five orders of magnitude reduction in permeability (Fossen and Bale, 2007). Cementation can also reduce permeability within the bands by up to five orders of magnitude in high-porosity rocks (e.g., Ogilvie and Glover, 2001) and can create baffles to fluid flow regardless of band type (e.g., Hesthammer et al., 2002). Pervasive cementation can also inhibit the formation of deformation bands by reducing the porosity of the host rock (Johansen et al., 2005).

Evidence of paleo-subsurface fluid flow is abundant in the layered sedimentary deposits within the equatorial regions of Mars (Ormö et al., 2004; McLennan et al., 2005; Grotzinger et al., 2005; Arvidson et al., 2006; Okubo and McEwen, 2007). The present-day extent of these deposits exceeds 3×10^6 km^2 within ±20° latitude of the equator alone (e.g., Schultz and Lutz, 1988; Hynek et al., 2003), and thicknesses range from ~600 m in Meridiani Terra to ~9 km in Valles Marineris (Hynek et al., 2003). Since these deposits appear to have undergone extensive erosion (e.g., Malin and Edgett, 2000, 2001; Hynek et al., 2003), their original extent was likely much greater. Thus, these deposits represent a potentially vast region of reservoir rock for subsurface fluids.

Formation of the equatorial layered deposits has been attributed to a variety of clastic sedimentary processes. Various deposits are interpreted as accumulations of eolian sediment (Scott and Tanaka, 1986; Greeley and Guest, 1987; Tanaka, 2000), pyroclastic material (Scott and Tanaka, 1982; Witbeck et al., 1991; Lucchitta et al., 1992; Murchie et al., 2000; Hynek et al., 2003), hyaloclastic debris (Chapman and Tanaka, 2001, 2002), lacustrine sediment (Witbeck et al., 1991; Lucchitta et al., 1992), and fluvial sediment (Malin and Edgett, 2003; Irwin et al., 2004; Quantin et al., 2005; Dromart et al., 2007).

Layered deposits examined by the Mars Exploration Rover (MER) *Opportunity* in Meridiani Planum (Fig. 2A) are sandstones of eolian to shallow fluvial origin (Grotzinger et al., 2005; McLennan and Grotzinger, 2008). These rocks consist of medium to coarse (0.2–1.0 mm) grains of roughly equal amounts of

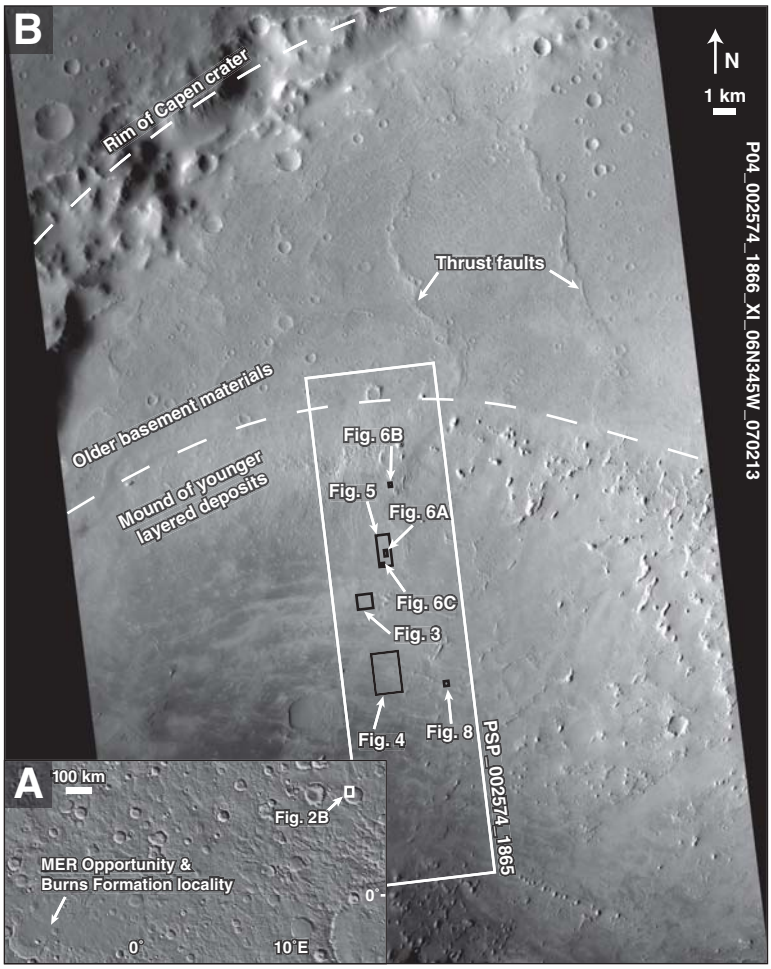

Figure 2. (A) Shaded relief map of the Arabia Terra region, Mars, showing the location of the deformation band focus area, which is located inside Capen crater centered at 6.67°N, 14.27°E (planetographic, IAU2000). This region contains numerous anastomosing ridges, which are the surface expressions of thrust fault–related folds. The location of Mars exploration Rover (MER) *Opportunity* is also shown. Illumination is from the upper right. Topography based on 128 pixel/degree Mars Orbiter Laser Altimeter (MOLA) gridded data. (B) Context Imager view of Capen crater. Figures 5 and 6 lie along the trace of a thrust fault–related fold that anastamoses through the upper right corner of the High-Resolution Imaging Science Experiment (HiRISE) scene. Folding of the layered deposits along the trace of the thrust fault is evident in stereo HiRISE imagery (PSP_002574_1865/PSP_003418_1865).

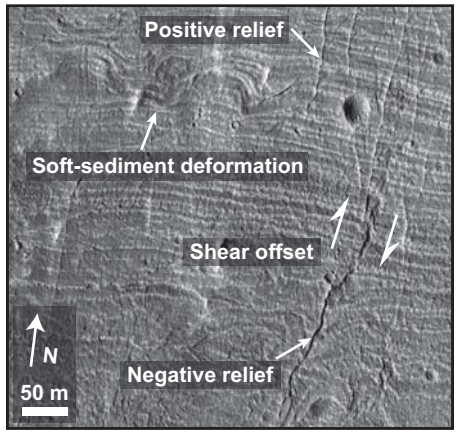

Figure 3. Evidence of soft-sediment deformation is widely observed within the study area. Subhorizontal banding is due to accumulations of dust along outcropping sedimentary layers. Stereo High-Resolution Imaging Science Experiment (HiRISE) views of the study area (PSP_002574_1865/PSP_003418_1865) indicate that this surface is essentially flat, and therefore layer undulations such as these are not due to topography. Also present are inosculating discontinuities that show varying amounts of shear displacement of cross-cut bedding. These discontinuities exhibit both positive and negative relief. Red channel image is from PSP_002574_1865. Illumination is from the left.

reworked evaporites and basaltic siliciclastic material, accompanied by varying amounts of cement (Herkenhoff et al., 2004; Grotzinger et al., 2005; McLennan et al., 2005; McLennan and Grotzinger, 2008).

Deformation bands are a prerequisite to faulting in porous and granular rocks (Wong et al., 1997; Schultz and Siddharthan, 2005; Aydin et al., 2006). Since much of the layered deposits are known or interpreted to consist of clastic sedimentary rocks, and since the layered deposits are faulted (e.g., Malin and Edgett, 2000; Okubo et al., 2007a), deformation bands can be expected to occur on Mars. Indeed, the presence of deformation band clusters on Mars has been previously proposed based on interpretations of low-resolution *Viking*, Mars Orbiter Laser Altimeter (MOLA), and Thermal Emission Imaging System (THEMIS) data (Artita and Schultz, 2005).

In this paper, we discuss the identification of deformation bands in recently available data collected by the High-Resolution Imaging Science Experiment (HiRISE) camera. HiRISE data offer one to two orders of magnitude increase in resolution over the data available in previous studies (Artita and Schultz, 2005). HiRISE images typically have 30 cm pixel widths and greater than 100:1 signal-to-noise ratios. Such high-resolution observations now enable the identification of deformation band clusters based on their characteristic meter-scale architectures, and they also allow diagenetic effects (e.g., cementation) to be accounted for when making this identification. These characteristic architectures, and evidence of diagenesis reported here, were unresolved in earlier Mars data. This paper presents archetypical examples of deformation band clusters from Arabia Terra, Mars, and summarizes the types of diagenetic features that are used to distinguish deformation bands from morphologically similar features such as joints and faults.

The findings reported here provide insight into timing for the deposition of the layered deposits and extant groundwater in the Arabia Terra region of Mars (Fig. 2A). Observed soft-sediment deformation structures in the layered deposits in Capen crater (Fig. 3) indicate

that groundwater was present there early on, perhaps during sediment deposition in an eolian dune and playa environment, as previously proposed for the Burns Formation (Grotzinger et al., 2005; Arvidson et al., 2006) in Meridiani Planum (Fig. 2A). Additionally, evidence of wall-rock induration indicates the presence of groundwater after some deformation band clusters had formed. The deformation band clusters are interpreted to be contemporaneous with the growth of several wrinkle ridges (thrust fault–related folds). Assuming that the deformation band clusters formed in the late Noachian to early Hesperian (4.0–3.5 Ga), during global wrinkle ridge formation (e.g., Tanaka et al., 1991; Watters, 1993; Dohm et al., 2001; Grott et al., 2007), accumulation of these layered deposits must have occurred prior to ca. 3.5 Ga, and it was contemporaneous with extant groundwater. These findings are consistent with interpretations of a pre-Hesperian age for these layered deposits, as well as a mid-Hesperian age for groundwater recession (Arvidson et al., 2006; Bibring et al., 2006; Andrews-Hanna et al., 2007).

DEFORMATION BANDS ON MARS

Deformation bands are especially well exposed on a mound of layered deposits within Capen crater, in south-central Arabia Terra (Fig. 2). Mounds of layered deposits such as this are common in impact craters in this region and may represent deeply eroded remnants of an extensive sheet of sediments that once blanketed the area (Malin and Edgett, 2000, 2001). Alternatively, these mounds may have grown in situ in the impact craters by extrusion of gas/water-sediment mixtures from the subsurface (e.g., Ori et al., 2000).

Erosional exposures offer clear views of distinct syn- and postdepositional structures that indicate the sedimentary nature of these layered deposits. Cross-bedding (100 m scale) is present (Fig. 4) and points to either eolian or subaqueous deposition. Soft-sediment deformation in the form of harmonic crenulations (Chan et al., 2007) is also present (Fig. 3), indicating that these sediments were water-saturated and subjected to synsedimentary deformation prior to lithification. Such observations are consistent with the interpretation that these layered deposits are composed of clastic sedimentary material.

These layered deposits are deformed by a series of north-south–trending thrust faults (wrinkle ridges; Fig. 2). The thrust faults deform the basement rock that forms the underlying impact crater, as well as the overlying mound of layered deposits. Exposed along the trace of the faults, there are numerous anastomosing discontinuities that crosscut bedding (Figs. 3–6; Figs. DR1 and DR2[1]). Individual discontinuities are thin (less than ~3 m wide), and they are tens of meters to roughly 3 k long. These structural discontinuities exhibit both positive and negative relief. Up to ~30 m of apparent horizontal offset of crosscut bedding is observed across the discontinuities. The clastic sedimentary nature of the host rock implies that this localized shear strain would have been accommodated through the formation of deformation bands. Localized shear strain may have also been accommodated along faults that subsequently nucleated within the deformation band clusters.

The structural discontinuities in Figures 3–6 (and Figs. DR1 and DR2 [see footnote 1]) exhibit map-view geometries that are consistent with clusters of deformation bands. The discontinuities show inosculating traces (compare Fig. 1B with Figs. 5, 6A, and 6B) that are a characteristic of individual deformation bands (Aydin, 1978; Aydin and Johnson, 1978) and clusters of bands (Davis, 1999) that have dip-slip shear displacements. These discontinuities

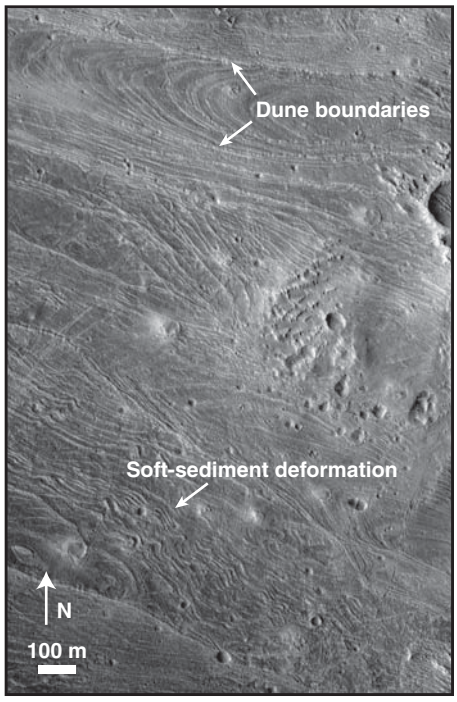

Figure 4. Cross-bedding is evident within these layered deposits. Boundaries between dune packets cross the image from roughly the upper left to the lower right. Evidence of soft-sediment deformation is also apparent. Stereo High-Resolution Imaging Science Experiment (HiRISE) views of the study area (PSP_002574_1865/PSP_003418_1865) show that these layer undulations are not due to the erosional expression of these deposits (i.e., the ground surface is essentially flat). Red channel and color mosaic are from PSP_002574_1865. Illumination is from the left.

Figure 5. Anastomosing discontinuities that are generally less than 3 m wide crosscut the sedimentary bedrock. Boundaries between dune sets within the sedimentary bedrock cross roughly right to left in this image. Shadow measurements indicate that these discontinuities form ridges that are generally <1 m high. Accumulations of light-toned dust highlight the meter-scale topography of the dark-toned bedrock and discontinuities. High-Resolution Imaging Science Experiment (HiRISE) color image is from PSP_002574_1865. Illumination is from the left.

[1]GSA Data Repository Item 2008191, supplemental figures, is available at www.geosociety.org/pubs/ft2008.htm. Requests may also be sent to editing@geosociety.org.

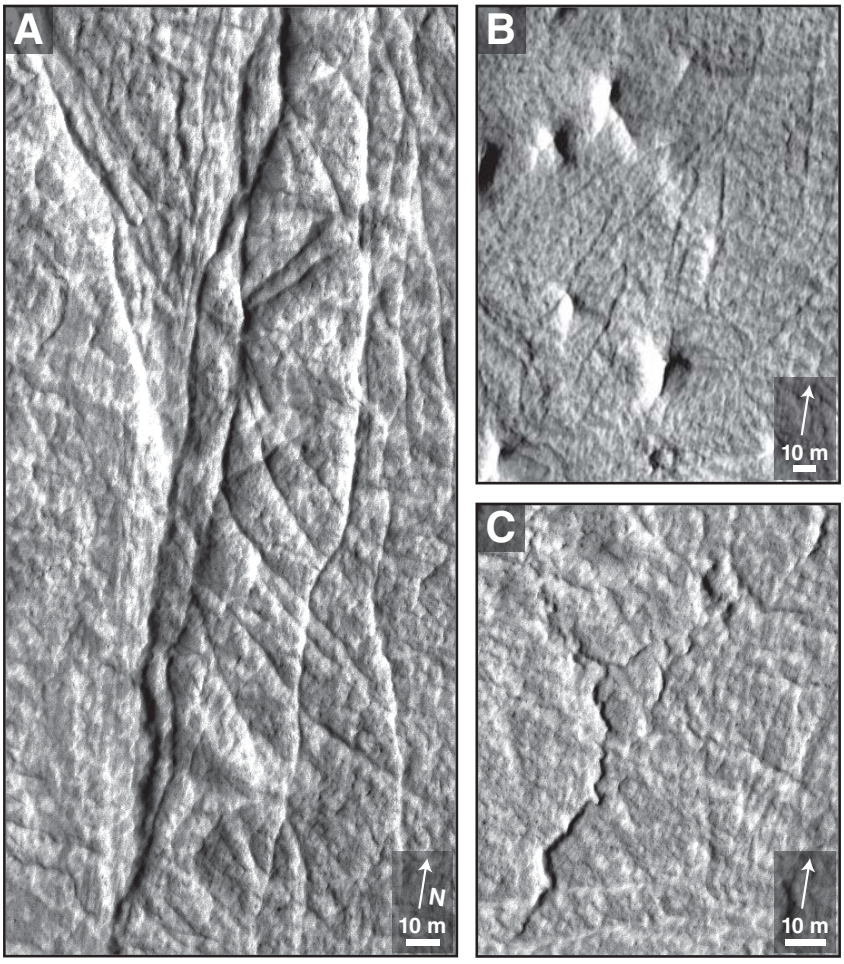

Figure 6. The discontinuities exhibit inosculating geometries in (A) positive relief and (B) negative relief. Discontinuities with crenulated geometries (C) are also present. Inosculating bands commonly exhibit shear offsets of crosscut bedding, while shear offsets are not apparent across discontinuities with crenulated geometries. Light-toned areas along the discontinuities are the result of accumulating dust rather than the result of diagenesis. High-Resolution Imaging Science Experiment (HiRISE) color image is from PSP_002574_1865. Locations of (A) and (C) are given in Figure 5. Location of (B) is given in Figure 2. Illumination is from the left.

occur along and are subparallel to the trace of thrust faults, consistent with a common driving stress field for both (e.g., Okubo and Schultz, 2005). Therefore, thrust displacements along these discontinuities are likely. Accordingly, the observed shear displacements of bedding (Figs. 3 and 6) are attributed to oblique exposures of thrust slip along these discontinuities.

Discontinuities that exhibit meter-scale crenulations and negligible shear, and which also crosscut bedding (Fig. 6C), are also present. This distinct geometry is consistent with the morphology of "compaction bands" (Mollema and Antonellini, 1996; Sternlof et al., 2005), a type of deformation band that forms with negligible shear strain.

Taken together, these lines of contextual and structural observations drive the interpretation that these discontinuities are clusters of deformation bands. This deformation is interpreted to have occurred at depth, after which the features were exhumed through erosion. The meter-scale widths of these discontinuities are consistent with the widths of deformation band clusters on Earth. Typical examples have millimeter-scale widths of individual deformation bands that would not be resolved in HiRISE images. The recognition of deformation band clusters is perhaps of greater significance than the identification of individual deformation bands because clusters of bands have a greater impact on fluid flow than individual bands do (e.g., Fossen and Bale, 2007).

The sense of volumetric strain along these deformation bands can be inferred from their erosional morphology as observed in terrestrial examples. Deformation bands commonly exhibit distinct erosional morphologies that reflect the sense of volumetric strain that they accommodate (Fig. 1). Dilational shear bands accommodate increases in intergranular pore space through breaking of grain-to-grain cements within the tabular thickness of the band. Thus, the rock within these bands is mechanically weaker than the surrounding host rock, and dilational shear bands can be expected, and are typically observed, to erode in negative relief (e.g., Okubo and Schultz, 2005). Compactional shear bands, on the other hand, form through loss of pore space due to increased grain-packing density and potentially cataclasis and pressure solution along grain contacts. Thus, compactional shear bands are more resistant to erosion than the host rock and typically erode in positive relief (e.g., Aydin, 1978; Mollema and Antonellini, 1996; Fossen et al., 2007). This general erosional morphology holds for the larger deformation band clusters as well, assuming negligible diagenesis.

Accordingly, the proposed deformation band clusters that have negative relief are interpreted to consist predominantly of dilational shear bands, whereas the positive-relief clusters are interpreted to primarily reflect localized compaction. An important caveat to this line of reasoning is that diagenetic cementation (e.g., Ogilvie and Glover, 2001) can cause discontinuities to erode in positive relief. Criteria to evaluate cementation along fractures (joints and faults) and deformation bands are discussed in the next section.

The identification of deformation bands on Mars is significant since these structures can influence the movement of subsurface fluids. The ability to distinguish deformation bands from fractures (i.e., sharp discontinuities such as faults and joints in crystalline rock) is key when utilizing models of deformation band growth around faults (e.g., Shipton et al., 2005; Okubo and Schultz, 2005; Fossen et al., 2007; Fossen and Bale, 2007) to investigate the impact of faulting on local patterns of fluid flow. Dilational shear bands can act as conduits to fluid flow since they form through localized increases in porosity and permeability. Compactional shear bands on the other hand can act as baffles to fluid flow since they form as a result of significant decreases in pore space and permeability. Therefore, at Capen crater, subsurface flow would be enhanced along the plane of the dilational shear bands, and flow would be impeded across the compactional shear bands (Figs. 3–7). Thus, these deformation bands would have acted to enhance local fluid flow in

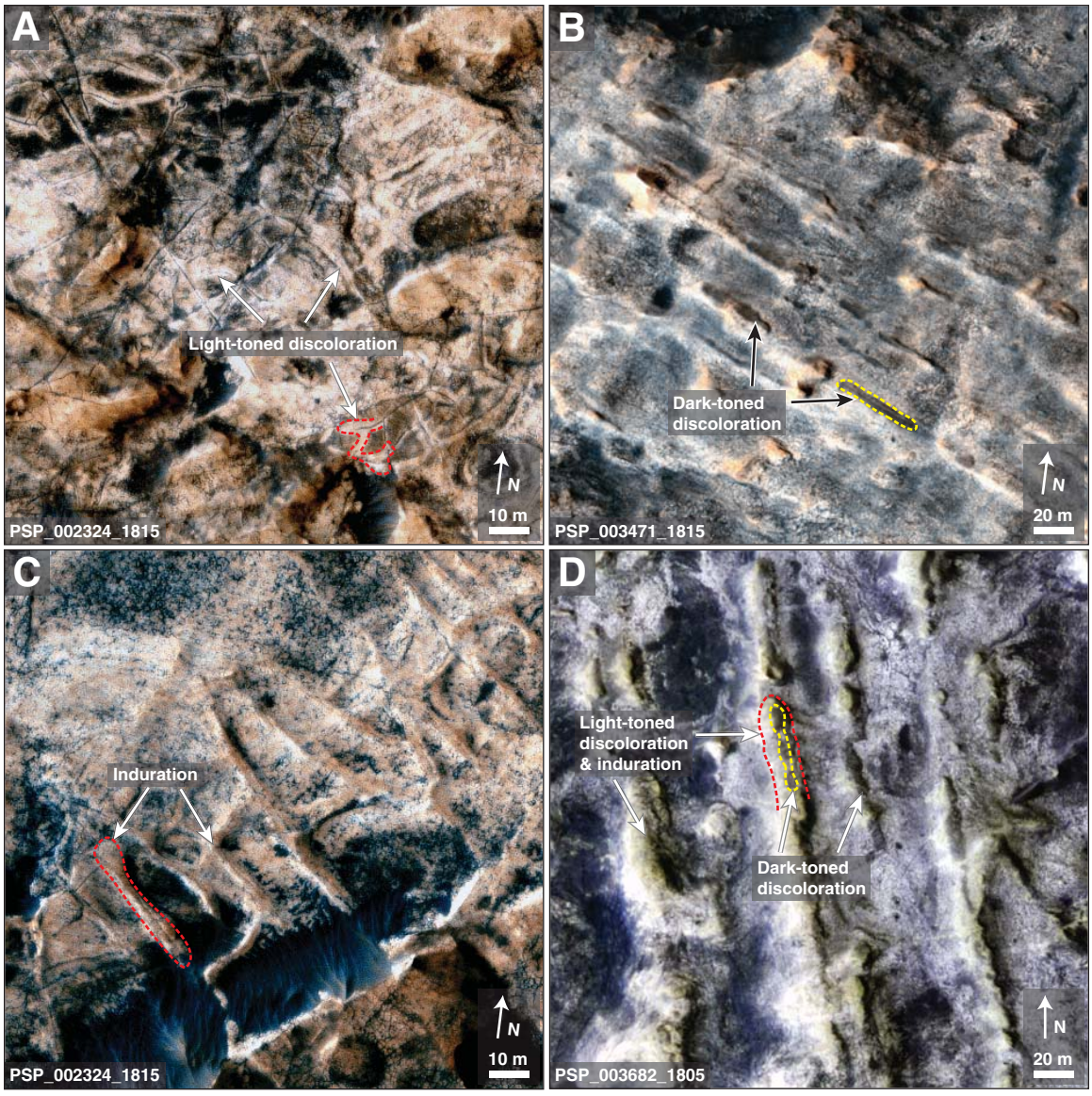

Figure 7. Examples of diagenesis along discontinuities in layered deposits in the Meridiani Planum area. Examples of each feature type are highlighted with a red (light-toned discoloration and wall-rock induration) or yellow (dark-toned discoloration) dashed line. (A) Apparent lightening in tone of the rock surrounding fractures. (B) Dark-toned discoloration along fractures. (C) Induration of the walls on either side of the fractures. The cleft formed by the fracture imparts a double-ridged morphology. (D) Dark-toned discoloration along light-toned ridges, which is attributed to overprinting of the diagenetic processes shown in (A)–(C). The light- and dark-toned patches of bedrock can be distinguished from topographic shading in stereo High-Resolution Imaging Science Experiment (HiRISE) images (Fig. DR3 [see text footnote 1]). Illumination is from the left in all images. Features such as these were proposed by Hynek et al. (2002) to be cemented fractures based on interpretations of Mars Orbiter Camera imagery.

a generally north-south direction and vertically through the layered sediments. Signs of diagenesis provide evidence of fluid flow along some of these deformation band clusters.

Deformation bands are differentiated from the fractures that form in crystalline rock based on the degree of strain localization (e.g., Aydin et al., 2006). Strain along deformation bands is distributed within the tabular thickness of the band and, to a lesser degree, within the surrounding host rock. Conversely, strain along faults and joints is accommodated at the sharp structural discontinuity that is the fracture wall. The style in which strain localizes in porous and granular (e.g., clastic sedimentary) rocks is influenced by the pervasiveness of cementation at the time of deformation. The trademarks of deformation band formation—changes in porosity, grain rolling, and grain crushing—are hindered by intergranular cements (e.g., Wong et al., 1997). Thus, in pervasively cemented sandstone (e.g., the Whatanga contact in the Burns Formation; McLennan, et al., 2005; Grotzinger et al., 2005), structural discontinuities behave mechanically as fractures do in crystalline rock rather than as deformation bands (e.g., Johansen et al., 2005). Therefore, characterization of the degree of cementation at the time of deformation is important when inferring the presence of deformation bands.

DIAGENETIC FINGERPRINTS

Prior to the arrival of HiRISE at Mars, orbiter-based evidence of structurally controlled fluid flow (flow along fractures and other geologic discontinuities) was limited to interpretations of imagery at greater than ~3–5 m resolution (e.g., Burr et al., 2002; Hynek et al., 2002; Ormö et al., 2004; Treiman, 2008) and was bolstered by strong mineralogic evidence of diagenesis and subsurface fluid flow (Christensen et al., 2000, 2001; Gendrin et al., 2005; Bibring et al., 2006). Data collected by MER *Opportunity* subsequently offered some of the strongest lines of evidence for subsurface fluid flow through the layered deposits in Meridiani Planum (McLennan et al., 2005; Squyres et al., 2006; Arvidson et al., 2006).

Light-toned halos along structural discontinuities (e.g., fractures and deformation bands) are commonly observed in HiRISE images of equatorial layered deposits (Fig. 7A). Such halos were initially observed in Candor Chasma (Okubo and McEwen, 2007). These halos are interpreted to reflect dissolution of dark-toned minerals, precipitation of light-toned minerals, or both, due to fluid flow along fractures. Precipitation of light-toned minerals may mask any dark-toned minerals within the host rock. Precipitated minerals may also help to preserve the appearance of a light-toned halo by indurating the host rock and thereby hindering the development of rough erosional surfaces that can act to trap dark-toned sand.

Conspicuous dark-toned patches were observed along structural discontinuities in many HiRISE images of equatorial layered deposits (e.g., Fig. 7B). Such features were not observed in the outcrops studied by Okubo and McEwen (2007). This discoloration is interpreted to be the result of grain coatings and cements of dark-toned minerals that have precipitated from fluids circulating along the discontinuity. Morphologically similar features have been interpreted as evidence of fluid flow on Earth (e.g., Eichhubl et al., 2004; Chan et al., 2000, 2005). These dark-toned discolorations are commonly localized at discrete points along discontinuities, suggesting that fluids were concentrated at structural stepovers where focused fluid flow can be expected.

HiRISE imagery also reveals that dark-toned discoloration of the host rock commonly occurs along discontinuities that are surrounded by light-toned halos (Figs. 7B and 7D; Fig. DR3 [see footnote 1]). This new observation indicates successive diagenetic events and demonstrates how temporal changes in groundwater chemistry can be recorded along structural discontinuities such as deformation band clusters (e.g., Parry et al., 2004). Thus, fluid flow along deformation bands and other discontinuities may be an important mechanism for concentrating hematite and other iron-bearing minerals within the layered deposits on Mars.

The processes of iron cycling (e.g., Parry et al., 2004; Chan et al., 2005, 2006; McLennan and Grotzinger, 2008; Tosca et al., 2008) and diagenetic recrystallization (McLennan et al., 2005; McLennan and Grotzinger, 2008) likely contribute to the changes in host-rock color along the fractures observed by Okubo and McEwen (2007) and in this paper. Iron cycling is likely given the abundances of iron minerals that are often detected (Geissler et al., 1993; Christensen et al., 2000, 2001; Arvidson et al., 2006; Farrand et al., 2007) in association with layered deposits. Recrystallization of evaporite minerals has been observed by MER *Opportunity* (e.g., McLennan et al., 2005; McLennan and Grotzinger, 2008) and can be expected in layered deposits that have a similar origin and geologic history.

Additionally, while Okubo and McEwen (2007) were unable to infer topographic evidence for wall-rock induration along the features they studied, discontinuities with a double-ridged morphology may be commonly observed in stereo HiRISE images (Figs. 7C and 8; see also anaglyph in Fig. DR2 [see footnote 1]). These discontinuities do not exhibit the clearly defined, meter-scale inosculations that are characteristic of deformation band clusters (Fig. 6). Instead, formation of these structures is attributed to induration of the wall rock on either side of the discontinuity. Accordingly, this double-ridged morphology is interpreted to be an indicator of preferential cementation (and fluid flow) along that discontinuity. The discontinuity may be a joint or a deformation band, depending on the degree of host-rock induration, and therefore strain localization, at the time of deformation. Pervasive cementation along the discontinuity is expected to mask any of the characteristic deformation band geometries. Therefore, classification of the discontinuity in remotely sensed data will be difficult if the degree of pretectonic diagenesis is unknown.

The alternative interpretations of the discontinuities shown in Figures 5 and 6 as either volcanic dikes or veins can be ruled out based

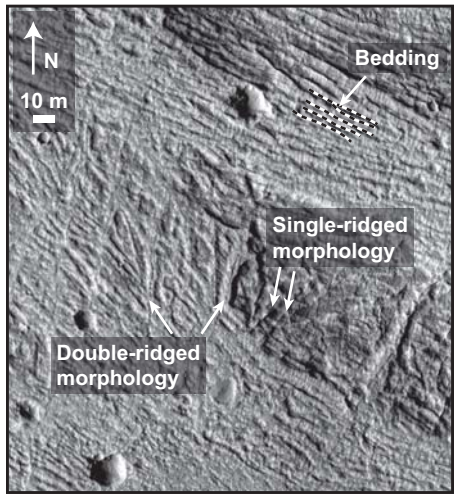

Figure 8. Evidence of wall-rock induration (cementation) along some bands in Capen crater is observed in the form of resistant ridges on either side of the fracture (see anaglyph in Fig. DR2 [see text footnote 1]). Compare this morphology with Figures 5, 6, and 7C. Single resistant ridges are clearly discernible from the double-ridged morphology. The single ridges are interpreted to be compactional shear bands with negligible wall-rock induration, while the double-ridged structures are interpreted to result from induration of the wall rock that bounds dilational shear bands. Bedding within the sedimentary bedrock crosses the image from roughly the upper left to the lower right. Red channel image is from PSP_002574_1865. Illumination is from the left.

on their observed widths and lengths (i.e., displacement-length scaling; Schultz et al., 2006, and references therein). An opening mode fracture (joint, dike, or vein) in layered deposits on Mars would have a width-to-length ratio of ~5×10^{-3} (Okubo et al., 2007b). For a discontinuity length of 3 km, 15 m of opening (width) would be expected if the discontinuity were a magmatic dike or vein. Instead, discontinuities of this length have a maximum observed width of ~3 m. Thus, the dimensions of the discontinuities are inconsistent with the critical strain required for a magmatic dike or vein. Additionally, dike material is not observed within these discontinuities as it is in other HiRISE images (e.g., PSP_004159_1660). Further, discoloration that may be evidence of fluid flow (e.g., Fig. 7), and that would support interpretations of veins, is also not observed along these discontinuities.

An origin as cataclastic dikes such as those observed in terrestrial impact craters (e.g., Kriens et al., 1999; Kenkmann, 2003) and in HiRISE images elsewhere (e.g., HiRISE image PSP_002682_1510) can also be ruled out. Cataclastic dikes originate as part of the parautochthonous breccia in the floor of impact craters. The outcrops studied here are within sediments that fill, and therefore postdate, the underlying Capen crater.

SUMMARY

We used basic principles of deformation band growth and morphology from terrestrial examples to interpret structural discontinuities observed in recent HiRISE images of Arabia Terra, Mars. Interpretations of deformation bands in orbital imagery, such as those made here, are reasonable where the host rock was likely porous and granular at the time of deformation. Structural discontinuities that cut diagenetic features, however, may behave as fractures if cementation is pervasive.

Diagenetic effects are herein accounted for when using apparent erosional morphology to infer the sense of volumetric strain along a deformation band. Preferential induration of the wall rock surrounding a discontinuity results in a double-ridged topographic expression of the band and the loss of clearly defined, meter-scale inosculations along it. This distinct double-ridged morphology is not apparent along the bands shown in Figures 5 and 6, and diagenetic alteration is therefore interpreted to be negligible. Evidence of wall-rock induration is however observed along adjacent bands (Fig. 8; Fig. DR2 [see footnote 1]). Comparisons of Figures 5–8 and Fig. DR2 show that cemented dilational shear bands may in this way be discerned from the single resistant ridge formed by compactional shear bands.

At Capen crater, the dark-toned bedrock shows no evidence of discoloration along the deformation band clusters (Fig. 6). A double-ridged morphology points to wall-rock induration along some, but not all, clusters (Fig. 8; Fig. DR2 [see footnote 1]). The clusters that contain evidence of induration are scattered amongst others that show no such evidence of cementation or discoloration. These variations in wall-rock induration suggest spatial differences in groundwater chemistry, terminal recession of groundwater during deformation band growth, or both. The apparent lack of discoloration may be the result of a lack of reactive fluids, a lack of primary dark-toned (e.g., iron) minerals in the bedrock, or these features may be obscured by the thin covering of light-toned dust that is pervasive throughout much of Arabia Terra.

Clusters of deformation bands and evidence of fluid flow along them (and other fractures) are now recognized in many HiRISE images of equatorial layered deposits. This work shows the importance of structural discontinuities in concentrating past diagenetic processes. Structural discontinuities are therefore recognized as key sites for furthering our understanding of past groundwater migration and chemistry throughout the equatorial layered deposits on Mars.

ACKNOWLEDGMENTS

We thank Haakon Fossen and an anonymous reviewer for comments that helped to improve this paper. This work was supported by a grant from the National Aeronautics and Space Administration (NASA) Mars Data Analysis Program to C.H. Okubo (05-MDAP05-0002).

REFERENCES CITED

Andrews-Hanna, J.C., Phillips, R.J., and Zuber, M.T., 2007, Meridiani Planum and the global hydrology of Mars: Nature, v. 446, p. 163–166, doi: 10.1038/nature05594.

Antonellini, M., and Aydin, A., 1994, Effect of faulting on fluid flow in porous sandstones; petrophysical properties: American Association of Petroleum Geologists Bulletin, v. 78, p. 355–377.

Antonellini, M., and Aydin, A., 1995, Effect of faulting on fluid flow in porous sandstones; geometry and spatial distribution: American Association of Petroleum Geologists Bulletin, v. 79, p. 642–671.

Artita, K.S., and Schultz, R.A., 2005, Significance of deformation band–like strike-slip faults on Mars: Houston, Lunar and Planetary Institute, 36th Lunar and Planetary Science Conference, abstract 2225.

Arvidson, R.E., et al., 2006, Nature and origin of the hematite-bearing plains of Meridiani Planum based on analyses of orbital and Mars Exploration Rover data sets: Journal of Geophysical Research, v. 111, E12S08, doi: 10.1029/2006JE002728.

Aydin, A., 1978, Small faults formed as deformation bands in sandstone: Pure and Applied Geophysics, v. 116, p. 913–930, doi: 10.1007/BF00876546.

Aydin, A., and Johnson, A.M., 1978, Development of faults as zones of deformation bands and as slip surfaces in sandstone: Pure and Applied Geophysics, v. 116, p. 931–942, doi: 10.1007/BF00876547.

Aydin, A., Borja, R.I., and Eichhubl, P., 2006, Geological and mathematical framework for failure modes in granular rock: Journal of Structural Geology, v. 28, p. 83–98, doi: 10.1016/j.jsg.2005.07.008.

Bibring, J.-P., et al., 2006, Global mineralogical and aqueous Mars history derived from OMEGA/Mars Express data: Science, v. 312, p. 400–404, doi: 10.1126/science.1122659.

Burr, D.M., Grier, J.A., McEwen, A.S., and Keszthelyi, L.P., 2002, Repeated aqueous flooding from the Cerberus Fossae: Evidence for very recently extant, deep groundwater on Mars: Icarus, v. 159, p. 53–73, doi: 10.1006/icar.2002.6921.

Chan, M.A., Parry, W.T., and Bowman, J.R., 2000, Diagenetic hematite and manganese oxides and fault-related fluid flow in Jurassic sandstones, southeastern Utah: American Association of Petroleum Geologists Bulletin, v. 84, p. 1281–1310, doi: 10.1306/A9673E82-1738-11D7-8645000102C1865D.

Chan, M.A., Beitler Bowen, B., Parry, W.T., Ormö, J., and Komatsu, G., 2005, Red rock and red planet diagenesis: Comparisons of Earth and Mars concretions: GSA Today, v. 15, no. 8, p. 4–10.

Chan, M.A., Johnson, C.M., Beard, B.L., Bowman, J.R., and Parry, W.T., 2006, Iron isotopes constrain the pathways and formation mechanisms of terrestrial oxide concretions: A tool for tracing iron cycling on Mars?: Geosphere, v. 7, p. 324–332.

Chan, M., Netoff, D., Blakey, R., Kocurek, G., and Alvarez, W., 2007, Clastic-injection pipes and syndepositional deformation structures in Jurassic eolian deposits: Examples from the Colorado Plateau, *in* Hurst, A., and Cartwright, J., eds., Sand Injectites: Implications for Hydrocarbon Exploration and Production: American Association of Petroleum Geologists (AAPG) Memoir 87, p. 233–244.

Chapman, M.G., and Tanaka, K.L., 2001, Interior trough deposits on Mars: Subice volcanoes?: Journal of Geophysical Research, v. 106, p. 10,087–10,100.

Chapman, M.G., and Tanaka, K.L., 2002, Related magma-ice interactions: Possible origins of chasmata, chaos and surface materials in Xanthe, Margaritifer, and Meridiani Terrae: Mars: Icarus, v. 155, p. 324–339.

Christensen, P.R., Bandfield, J.L., Clark, R.N., Edgett, K.S., Hamilton, V.E., Hoefen, T., Kieffer, H.H., Kuzmin, R.O., Lane, M.D., Malin, M.C., Morris, R.V., Pearl, J.C., Pearson, R., Roush, T.L., Ruff, S.W., and Smith, M.D., 2000, Detection of crystalline hematite mineralization on Mars by the Thermal Emission Spectrometer: Evidence for near-surface water: Journal of Geophysical Research, v. 105, no. E4, p. 9623–9642, doi: 10.1029/1999JE001093.

Christensen, P.R., Morris, R.V., Lane, M.D., Bandfield, J.L., and Malin, M.C., 2001, Global mapping of Martian hematite mineral deposits: Remnants of water-driven processes on early Mars: Journal of Geophysical Research, v. 106, p. 23,873–23,886, doi: 10.1029/2000JE001415.

Davis, G.H., 1999, Structural Geology of the Colorado Plateau Region of Southern Utah, with Special Emphasis on Deformation Bands: Geological Society of America Special Paper 342, 157 p.

Dohm, J.M., Takana, K.L., and Hare, T.M., 2001, Paleotectonic Map of the Thaumasia Region, Mars: U.S. Geological Survey Geological Investigations Series I-2650, scale 1:5,000,000.

Dromart, G., Quantin, C., and Broucke, O., 2007, Stratigraphic architectures spotted in southern Melas Chasma, Valles Marineris, Mars: Geology, v. 35, p. 363–366, doi: 10.1130/G23350A.1.

Eichhubl, P., Taylor, W.L., Pollard, D.D., and Aydin, A., 2004, Paleo–fluid flow and deformation in the Aztec Sandstone at the Valley of Fire, Nevada—Evidence for the coupling of hydrogeologic, diagenetic, and tectonic processes: Geological Society of America Bulletin, v. 116, p. 1120–1136, doi: 10.1130/B25446.1.

Farrand, W.H., Bell III, J.F., Johnson, J.R., Jolliff, B.L., Knoll, A.H., McLennan, S.M., Squyres, S.W., Calvin, W.M., Grotzinger, J.P., Morris, R.V., Soderblom, J., Thompson, S.D., Watters, W.A., and Yen, A.S., 2007, Visible and near-infrared multispectral analysis of rocks at Meridiani Planum, Mars, by the Mars Exploration

Rover *Opportunity*: Journal of Geophysical Research, v. 112, E06S02, doi: 10.1029/2006JE002773.

Fossen, H., and Bale, A., 2007, Deformation bands and their influence on fluid flow: American Association of Petroleum Geologists Bulletin, v. 91, p. 1685–1700, doi: 10.1306/07300706146.

Fossen, H., Johansen, T.E.S., Rotevatn, A., and Hesthammer, J., 2005, Fault interaction in porous sandstones: American Association of Petroleum Geologists Bulletin, v. 89, p. 1593–1606, doi: 10.1306/07290505041.

Fossen, H., Schultz, R.A., Shipton, Z., and Mair, K., 2007, Deformation bands in sandstone—A review: Journal of the Geological Society of London, v. 164, p. 755–769, doi: 10.1144/0016-76492006-036.

Geissler, P.E., Singer, R.B., Komatsu, G., Murchie, S., and Mustard, J., 1993, An unusual spectral unit in west Candor Chasma: Evidence for aqueous or hydrothermal alteration in the Martian canyons: Icarus, v. 106, p. 380–391, doi: 10.1006/icar.1993.1179.

Gendrin, A., Mangold, N., Bibring, J-P., Langevin, Y., Gondet, B., Poulet, F., Bonello, G., Quantin, C., Mustard, J., Arvidson, R., and LeMouélic, S., 2005, Sulfates in Martian layered terrains: The OMEGA/Mars Express view: Science, v. 307, p. 1587–1591, doi: 10.1126/science.1109087.

Greeley, R., and Guest, J.E., 1987, Geologic Map of the Eastern Equatorial Region of Mars: U.S. Geological Survey Miscellaneous Investigation Series Map I-1802-B, scale 1:15,000,000, 1 sheet.

Grott, M., Hauber, E., Werner, S.C., Kronberg, P., and Neukum, G., 2007, Mechanical modeling of thrust faults in the Thaumasia region, Mars, and implications for the Noachian heat flux: Icarus, v. 186, p. 517–526, doi: 10.1016/j.icarus.2006.10.001.

Grotzinger, J.P., et al., 2005, Stratigraphy and sedimentology of a dry to wet eolian depositional system, Burns Formation, Meridiani Planum: Mars: Earth and Planetary Science Letters, v. 240, p. 11–72, doi: 10.1016/j.epsl.2005.09.039.

Herkenhoff, K.E., et al., 2004, Evidence from *Opportunity*'s microscopic imager for water on Meridiani Planum: Science, v. 306, p. 1727–1730.

Hesthammer, J., Bjorkum, P.A., and Watts, L., 2002, The effect of temperature on sealing capacity of faults in sandstone reservoirs: Examples from the Gullfaks and Gullfaks Sor fields: American Association of Petroleum Geologists Bulletin, v. 86, p. 1733–1751.

Hynek, B.M., Arvidson, R.E., and Phillips, R.J., 2002, Geologic setting and origin of Meridiani Planum hematite deposit on Mars: Journal of Geophysical Research, v. 107, p. 5088, doi: 10.1029/2002JE001891.

Hynek, B.M., Phillips, R.J., and Arvidson, R.E., 2003, Explosive volcanism in the Tharsis region: Global evidence in the Martian geologic record: Journal of Geophysical Research, v. 108, p. 5111, doi: 10.1029/2003JE002062.

Irwin, R.P., Howard, A.D., and Maxwell, T.A., 2004, Geomorphology of Ma'adim Vallis, Mars, and associated paleolake basins: Journal of Geophysical Research, v. 109, E12009, doi: 10.1029/2004JE002287.

Johansen, T.E.S., Fossen, H., and Kluge, R., 2005, The impact of syn-faulting porosity on damage zone architecture in porous sandstone: An outcrop example from the Moab fault, Utah: Journal of Structural Geology, v. 27, p. 1469–1485, doi: 10.1016/j.jsg.2005.01.014.

Kenkmann, T., 2003, Dike formation, cataclastic flow, and rock fluidization during impact cratering: An example from the Upheaval Dome structure, Utah: Earth and Planetary Science Letters, v. 214, p. 43–58.

Kriens, B., Shoemaker, E., and Herkenhoff, K., 1999, Geology of the Upheaval Dome impact structure, southeast Utah: Journal of Geophysical Research, v. 104, p. 18,867–18,887.

Lucchitta, B.K., McEwen, A.S., Clow, G.D., Geissler, P.E., Singer, R.B., Schultz, R.A., and Squyres, S.W., 1992, The canyon system on Mars, *in* Kieffer, H.H., et al., eds., Mars: Tucson, University of Arizona Press, p. 423–492.

Malin, M.C., and Edgett, K.S., 2000, Sedimentary rocks of early Mars: Science, v. 290, p. 1927–1937, doi: 10.1126/science.290.5498.1927.

Malin, M.C., and Edgett, K.S., 2001, Global Surveyor Mars Orbiter Camera: Interplanetary cruise through primary mission: Journal of Geophysical Research, v. 106, p. 23,429–23,570.

Malin, M.C., and Edgett, K.S., 2003, Evidence for persistent flow and aqueous sedimentation on early Mars: Science, v. 302, p. 1931–1934.

McLennan, S.M., and Grotzinger, J.P., 2008, The sedimentary rock cycle of Mars, *in* Bell, J.F., ed., The Martian Surface: Composition, Mineralogy, and Physical Properties: New York, Cambridge University Press, p. 541–577.

McLennan, S.M., et al., 2005, Provenance and diagenesis of the evaporite-bearing Burns Formation, Meridiani Planum: Mars: Earth and Planetary Science Letters, v. 240, p. 95–121, doi: 10.1016/j.epsl.2005.09.041.

Mollema, P.N., and Antonellini, M.A., 1996, Compaction bands: A structural analog for anti-mode I cracks in aeolian sandstone: Tectonophysics, v. 267, p. 209–228, doi: 10.1016/S0040-1951(96)00098-4.

Murchie, S., Kirkland, L., Erard, S., Mustard, J., and Robinson, M., 2000, Near-infrared spectral variations of Martian surface materials from ISM imaging spectrometer data: Icarus, v. 147, p. 444–471.

Ogilvie, S.R., and Glover, P.W.J., 2001, The petrophysical properties of deformation bands in relation to their microstructure: Earth and Planetary Science Letters, v. 193, p. 129–142, doi:10.1016/S0012-821X(01)00492-7.

Okubo, C.H., and McEwen, A.S., 2007, Fracture controlled paleo–fluid flow in Candor Chasma, Mars: Science, v. 315, p. 983–985, doi: 10.1126/science.1136855.

Okubo, C.H., and Schultz, R.A., 2005, Evolution of cluster geometry and intensity in porous sandstone: Insight from strain energy density: Journal of the Geological Society of London, v. 162, p. 939–949, doi: 10.1144/0016-764904-148.

Okubo, C.H., Lewis, K., McEwen, A.S., Kirk, R., and The HiRISE Team, 2007a, High-resolution structural mapping in southwest Candor Chasma: Eos (Transactions, American Geophysical Union), v. 88, abstract P23D-06.

Okubo, C.H., Schultz, R.A., Polit, A.T., McEwen, A.S., and The HiRISE Team, 2007b, Displacement-length scaling of joints in layered deposits, southwest Candor Chasma: Houston, Lunar and Planetary institute, 38th Lunar and Planetary Science Conference, abstract 1225.

Ori, G.G., Marinangeli, L., and Komatsu, G., 2000, Gas (methane)–related features on the surface of Mars and subsurface reservoirs: Houston, Lunar and Planetary institute, 31st Lunar and Planetary Science Conference, abstract 1550.

Ormö, J., Komatsu, G., Chan, M.A., Beitler, B., and Parry, W.T., 2004, Geological features indicative of processes related to the hematite formation in Meridiani Planum and Aram Chaos, Mars: A comparison with diagenetic hematite deposits in southern Utah, USA: Icarus, v. 171, p. 295–316, doi: 10.1016/j.icarus.2004.06.001.

Parry, W.T., Chan, M.A., and Beitler, B., 2004, Chemical bleaching indicates episodes of fluid flow in deformation bands in sandstone: American Association of Petroleum Geologists Bulletin, v. 88, p. 175–191, doi: 10.1306/09090303034.

Quantin, C., Allemand, P., Mangold, N., Dromart, G., and Delacourt, C., 2005, Fluvial and lacustrine activity on layered deposits in Melas Chasma, Valles Marineris: Mars: Journal of Geophysical Research, v. 110, E12S19, doi: 10.1029/2005JE002440.

Schultz, P.H., and Lutz, A.B., 1988, Polar wandering of Mars: Icarus, v. 73, p. 91–141.

Schultz, R.A., and Balasko, C.M., 2003, Growth of deformation bands into echelon and ladder geometries: Geophysical Research Letters, v. 30, p. 2033, doi: 10.1029/2002GL018449.

Schultz, R.A., and Fossen, H., 2008, Terminology for structural discontinuities: American Association of Petroleum Geologists Bulletin, v. 92, p. 853–867, doi: 10.1306/02200807065.

Schultz, R.A., and Siddharthan, R., 2005, A general framework for the occurrence and faulting of deformation bands in porous granular rocks: Tectonophysics, v. 411, p. 1–18, doi: 10.1016/j.tecto.2005.07.008.

Schultz, R.A., Okubo, C.H., and Wilkins, S.J., 2006, Displacement-length scaling relations for faults on the terrestrial planets: Journal of Structural Geology, v. 28, p. 2182–2193, doi: 10.1016/j.jsg.2006.03.034.

Scott, D.H., and Tanaka, K.L., 1982, Ignimbrites of Amazonis Planitia region of Mars: Journal of Geophysical Research, v. 87, p. 1179–1190.

Scott, D.H., and Tanaka, K.L., 1986, Geologic Map of the Western Equatorial Region of Mars: U.S. Geological Survey Miscellaneous Investigation Series Map I-1802-A, scale 1:15,000,000, 1 sheet.

Shipton, Z.K., Evans, J.P., and Thompson, L.B., 2005, The geometry and thickness of deformation band fault core, and its influence on sealing characteristics of deformation band fault zones, *in* Sorkhabi, R., and Tusuji, Y., eds., Faults, Fluid Flow and Petroleum Traps: American Association of Petroleum Geologists (AAPG) Memoir 85, p. 181–195.

Squyres, S.W., Knoll, A.H., Arvidson, R.E., Clark, B.C., Grotzinger, J.P., Jolliff, B.L., McLennan, S.M., Tosca, N., Bell III, J.F., Calvin, W.M., Farrand, W.H., Glotch, T.D., Golombek, M.P., Herkenhoff, K.E., Johnson, J.R., Klingelhöfer, G., McSween, H.Y., and Yen, A.S., 2006, Two years at Meridiani Planum: Results from the *Opportunity* rover: Science, v. 313, p. 1403–1407, doi: 10.1126/science.1130890.

Sternlof, K.R., Rudnicki, J.W., and Pollard, D.D., 2005, Anticrack inclusion model for compaction bands in sandstone: Journal of Geophysical Research, v. 110, p. B11403, doi: 10.1029/2005JB003764.

Tanaka, K.L., 2000, Dust and ice deposition in the Martian geologic record: Icarus, v. 144, p. 254–266.

Tanaka, K.L., Golombek, M.P., and Banerdt, W.B., 1991, Reconciliation of stress and structural histories of the Tharsis region of Mars: Journal of Geophysical Research, v. 96, p. 15,617–15,633.

Taylor, W.L., and Pollard, D.D., 2000, Estimation of in situ permeability of deformation bands in porous sandstone, Valley of Fire, Nevada: Water Resources Research, v. 36, p. 2595–2606, doi: 10.1029/2000WR900120.

Tosca, N.J., McLennan, S.M., Dyar, M.D., Sklute, E.C., and Michel, F.M., 2008, Fe oxidation processes at Meridiani Planum and implications for secondary Fe mineralogy on Mars: Journal of Geophysical Research, v. 113, p. E05005, doi: 10.1029/2007JE003019.

Treiman, A.H., 2007, Ancient groundwater flow in the Valles marineris on Mars inferred from fault trace ridges: Nature Geoscience, v. 1, 181–183, doi: 10.1038/ngeo131.

Watters, T.R., 1993, Compressional tectonism on Mars: Journal of Geophysical Research, v. 98, p. 17,049–17,060.

Witbeck, N.E., Tanaka, K.L., and Scott, D.H., 1991, Geologic Map of the Valles Marineris Region, Mars: U.S. Geological Survey Miscellaneous Investigation Series Map I-2010, scale 1:2,000,000, 1 sheet.

Wong, T-f., David, C., and Zhu, W., 1997, The transition from brittle faulting to cataclastic flow in porous sandstones: Mechanical deformation: Journal of Geophysical Research, v. 102, p. 3009–3025, doi: 10.1029/96JB03281.

Manuscript Received 23 February 2008
Revised Manuscript Received 28 May 2008
Manuscript Accepted 19 June 2008

Printed in the USA